Synthesis and Characterization of Hybrid Porphyrin Dimers and Halogenated Porphyrin Dimers

Kouji Iida, Mamoru Nango,* Kenichi Okada, Masaya Hikita, Mitsutaka Matsuura, Takayuki Kurihara, Takeharu Tajima, Ayako Hattori, Shinichi Ishikawa, Keiji Yamashita, Kazuichi Tsuda,* and Yukihisa Kurono†

Department of Applied Chemistry, Nagoya Institute of Technology, Gokiso-cho, Showa-ku, Nagoya 466

†Department of Pharmaceutics, Faculty of Pharmaceutical Sciences, Nagoya City University, 3-1 Tanabe-dori, Mizuho-ku, Nagoya 467

(Received August 29, 1994)

Zinc hybrid porphyrin dimer(ZnTTP-C_2-H_2PFPP, ZnTTP-C_2-H_2TTP, ZnPFPP-C_2-H_2PFPP, and ZnPFPP-C_2-H_2TTP) and manganese (III) halogenated porphyrin dimers (MnPFPP-C_2-MnPFPP, MnPFPP-C_2-MnDCPP, and MnDCPP-C_2-MnDCPP) covalently bridged by an ethylene moiety (Scheme 1) were synthesized and characterized by UV-vis spectra, fluorescence spectra, and cyclic voltammograms. These porphyrin dimers could be embedded into the lipid bilayers of a liposomal membrane. The redox potential of the manganese complex for the halogenated porphyrin dimers increased with increasing of halogen portions on the porphyrin rings. An efficient energy transfer of the excited singlet state in the covalently-linked zinc hybrid dimers from zinc porphyrin to a free base porphyrin was observed, depending on the porphyrin structure. Furthermore, the manganese halogenated porphyrin dimers acted as catalysts of transmembrane electron transfer; such activity depends on the steric effect of halogen portions on the porphyrin ring.

Synthetic porphyrin models can be helpful in studying the effect of porphyrin structure in electron transfer reactions of biological processes.[1—4] Porphyrin pigments play a key role in the electron transfer in photosynthetic and mitochondorial membranes.[5] Many porphyrin derivatives were studied as models of charge separation and recombination which are involved in early photosynthesis events. The study of well-defined, covalently-linked dimer,[6,7] trimer,[8] and tetramer[9] complexes will be required in order to understand these primary electron donor units, such as the light harvesting complexes in photosynthetic bacteria. Covalently-linked porphyrin dimers are also being studied as models for electron transport reactions between metalloporphyrin centers in P-450[10] mimicking reactions in oxidative metabolism.[11] However, there has been little study of ground state electron transfer between porphyrin complexes to provide an insight into the effect of porphyrin structure in these electron transfer reactions in lipid bilayers.[1] Use of covalently-linked halogenated porphyrin complexes as model systems for these electron transfers promises to lead to a greater understanding of these important reactions.

In this paper, we report the synthesis of halogenated porphyrin dimers (Scheme 1), the characterization of these porphyrin complexes, and their interactions with lipid bilayers of liposomal membrane by using UV-vis spectra, fluorescence spectra, and cyclic voltammograms. We reasoned that the halogenated porphyrins are stable against oxidant and exhibit unique reactivities because of the steric and electron-withdrawing effects of halogen portions on the porphyrin ring.[2,3] In addition, the covalently-linked two porphyrin centers should allow more possibility for electron transfer than the monomer porphyrin.[4] An energy transfer of the excited singlet state in the covalently-linked zinc hybrid dimers from zinc porphyrin to a free base porphyrin is examined to study the effect of the structure and redox potential of these complexes on the energy transfer. Furthermore, transmembrane electron transfer catalyzed by manganese(III) halogenated porphyrin dimers is preliminarily studied to provide an insight into the effect of porphyrin structure in the electron transfer reaction.

Experimental

All reactions and chromatographic separations were carried out in minimum room light. Benzene, chloroform, dichloromethane, and pyridine were distilled and then stored over molecular sieves. Other solvents used were guaranteed grade or spectral grade. Bis(2,4-pentanedionato) manganese(II) was obtained from Ventron Co. The silica gel used for dry column chromatography was ICN Absorbentien 04526 and 04580 (ICN BIOMEDICALS). Merck DC-Plastik-

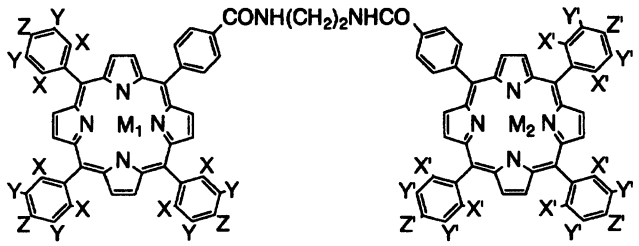

M_1P_1-C_2-M_2P_2	P_1	P_2	M_1	M_2	X	Y	Z	X'	Y'	Z'
H_2PFPP-C_2-H_2PFPP	PFPP	PFPP	H_2	H_2	F	F	F	F	F	F
H_2PFPP-C_2-H_2DCPP	PFPP	DCPP	H_2	H_2	F	F	F	Cl	H	H
H_2PFPP-C_2-H_2TTP	PFPP	TTP	H_2	H_2	F	F	F	H	H	Me
ZnTTP-C_2-H_2PFPP	TTP	PFPP	Zn	H_2	H	H	Me	F	F	F
ZnTTP-C_2-H_2TTP	TTP	TTP	Zn	H_2	H	H	Me	H	H	Me
ZnPFPP-C_2-H_2PFPP	PFPP	PFPP	Zn	H_2	F	F	F	F	F	F
ZnPFPP-C_2-H_2TTP	PFPP	TTP	Zn	H_2	F	F	F	H	H	Me
MnPFPP-C_2-MnPFPP	PFPP	PFPP	Mn	Mn	F	F	F	F	F	F
MnPFPP-C_2-MnDCPP	PFPP	DCPP	Mn	Mn	F	F	F	Cl	H	H
MnDCPP-C_2-MnDCPP	DCPP	DCPP	Mn	Mn	Cl	H	H	Cl	H	H
MnPFPP-C_2-H_2PFPP	PFPP	PFPP	Mn	H_2	F	F	F	F	F	F
MnTTP-C_2-MnP(COOMe)$_3$	TTP	P(COOMe)$_3$	Mn	Mn	H	H	Me	H	H	COOMe

Scheme 1. Halogenated porphyrin dimers.

folien kiesel-gel 60F_{254} and Merck DC-Fertigplatten kieselgel 60 were used for analytical and preparative thin-layer chromatography, respectively. Egg yolk phosphatidylcholine (egg PC) was obtained from Nippon Fine Chemical Co.

Synthetic Procedures. 5,10,15,20-Tetrakis(*p*-tolyl)-porphyrin (H_2TTP), 5-(4-methoxycarbonyphenyl)-10,15,20-tri(*p*-tolyl)porphyrin (H_2TTPCOOMe), 5-(4-carboxyphenyl)-10,15,20-tri(*p*-tolyl)porphyrin (H_2TTPCOOH), 5-(4-carboxyphenyl)-10,15,20-tris(4-carbomethoxyphenyl)porphyrin (H_2P(COOMe)$_3$COOH), and their zinc or manganese(III) complexes were prepared as described previously.[1,12]

5,10,15,20-Tetrakis(pentafluorophenyl)porphyrin (H_2PFPP); 5-(4-Methoxycarbonylphenyl)-10,15,20-tris(pentafluorophenyl)porphyrin (H_2PFPPCOOMe); 5,10,15,20-Tetrakis(2,6-dichlorophenyl)porphyrin (H_2DCPP); and 5-(4-Methoxycarbonylphenyl)-10,15,20-tris(2,6-dichlorophenyl)porphyrin (H_2DCPPCOOMe). These compounds were prepared by a literature method.[13] As an example, the synthesis of H_2PFPPCOOMe will be described. 1.40 ml of pyrrole (20 mmol), 1.92 ml of pentafluorobenzaldehyde (16 mmol) and 656 mg of 4-methoxycarbonylbenzaldehyde (4 mmol) were dissolved in dichloromethane (800 ml) and degassed by nitrogen for 30 min. Then 0.30 ml of diethylether–boron trifluoride (1/1) was added and the solution was stirred for 40 h at 37 °C. Then 3.7 mg of chloranil (15 mmol) was added and the solution was stirred for 3 h at 37 °C. The dichloromethane was removed under reduced pressure and the sample was purified by silica gel chromatography with chloroform : hexane=2 : 3 as eluent. The first eluent was H_2PFPP and the second eluent was H_2PFPPCOOMe. The yields were 30% (1.3 g) and 44% (1.7 g), respectively.

H_2PFPP: ^{1}H NMR ($CDCl_3$) δ=−2.92 (2H, s, pyrrole-NH), 8.96 (8H, s, pyrrole-β-H); UV (CH_2Cl_2–10%EtOH) λ_{max} 410 nm (ε 208 $mM^{-1}cm^{-1}$) (M=mol dm^{-3}), 505 (15.6), 582 (5.06); Emission λ_{max} (Ex.=412.5 nm) (CH_2Cl_2–10%EtOH) 638 nm, 704; MS (FAB) *m/z* 975 (MH^+).

H_2PFPPCOOMe: ^{1}H NMR ($CDCl_3$) δ=−2.92 (2H, s, pyrrole-NH), 4.2 (3H, s, ester-Me), 8.3 (2H, d, Ar 3-H and 5-H), 8.5 (2H, d, Ar 2-H and 6-H), 8.8 (2H, s, pyrrole-β-H), 8.9 (6H, s, β pyrrole); UV (CH_2Cl_2–10%EtOH) λ_{max} 412.5 nm (ε 327 $mM^{-1}cm^{-1}$), 506.5 (27.1), 584 (9.83); Emission λ_{max} (Ex.=412.5 nm) (benzene–1% pyridine) 646 nm, 711; MS (FAB) *m/z* 943 (MH^+).

H_2DCPP: The yield was 10%. ^{1}H NMR ($CDCl_3$) δ=−2.6 (2H, s, pyrrole-NH), 7.6—7.8 (12H, m, 2,6-dichlorophenyl 3-H, 4-H, and 5H), 8.7 (8H, s, pyrrole-β-H); UV (CH_2Cl_2–10%EtOH) λ_{max} 418 nm, 502, 565, 604; MS (FAB) 890 (MH^+ for 7 ^{35}Cl and 1 ^{37}Cl).

H_2DCPPCOOMe: The yield was 35%. ^{1}H NMR ($CDCl_3$) δ=−2.6 (2H, s, pyrrole-NH), 4.1 (3H, s, ester-Me), 7.6—7.8 (9H, m, 2,6-dichlorophenyl 3-H, 4-H, and 5H), 8.3 (2H, d, 4-methoxycarbonylphenyl 3-H and 5-H), 8.4 (2H, d, 4-methoxycarbonylphenyl 2-H and 6-H), 8.7 (6H, s, β pyrrole), 8.8 (2H, s, β pyrrole); UV (CH_2Cl_2–10%EtOH) λ_{max} 417 nm (ε 400 $mM^{-1}cm^{-1}$), 512 (23.5), 589 (7.64); Emission (CH_2Cl_2–10%EtOH) λ_{max} (Ex.=417 nm) 649.5 nm, 713.5; MS (FAB) *m/z* 880 (MH^+ for 4 ^{35}Cl and 2 ^{37}Cl).

5-(4-Carboxylphenyl)-10,15,20-tris(pentafluorophenyl)porphyrin (H_2PFPPCOOH). One gram of PFPPCOOMe (1.07 mmol) was dissolved in THF (60 ml) and 2 M KOH in H_2O (60 ml) was added. The mixture was stirred at 40 °C overnight in the dark. The cooled solution was then acidified with 2 M HCl to pH 4, and 0.25 M aqueous ammonia was added to pH 8.0. Then 200 ml of chloroform and 300 ml of distilled water were added. The purple precipitates which appeared were extracted into chloroform. The combined extracts were washed twice with water, then dried over $MgSO_4$; the solvent was removed under reduced pressure. The sample was purified by silica gel chromatography with chloroform : acetone=4 : 1 as eluent. The yield of H_2PFPPCOOH was 67% (665 mg).

^{1}H NMR ($CDCl_3$) δ=−2.9 (2H, s, pyrrole-NH), 8.3 (2H, s, Ar 3-H and 5-H), 8.5 (2H, s, Ar 2-H and 6-H), 8.8 (2H, s, pyrrole-β-H), 8.9 (6H, s, pyrrole-β-H); MS (FAB) *m/z* 929 (MH^+).

5-(4-Carboxylphenyl)-10,15,20-tris(2,6-dichloro-

phenyl)-porphyrin (H_2DCPPCOOH). ^{1}H NMR ($CDCl_3$) $\delta=-2.6$ (2H, s, pyrrole-NH), 7.6—7.8 (9H, m, 2, 6-dichlorophenyl 3-H, 4-H, and 5H), 8.3 (2H, d, 4-methoxycarbonylphenyl 3-H, and 5H), 8.4 (2H, d, 4-methoxycarbonylphenyl 2-H and 6H), 8.7 (2H, s, pyrrole-β-H), 8.8 (6H, s, pyrrole-β-H); MS (FAB) m/z 865 (MH^+).

H_2PFPP-C_2-H_2PFPP: First 400 mg of H_2PFPPCOOH (0.432 mmol) was dissolved in dry benzene (40 ml). Then 4.6 ml of thionyl chloride (50 mmol) was added and the solution was brought to reflux for 1.5 h. The residue was redissolved in benzene (15 ml) and once again taken to dryness under reduced pressure to remove traces of thionyl chloride. The acid chloride was redissolved in chloroform, and 2 drops of triethylamine and ethylenediamine (0.216 mmol) was added. The sample was purified by silica gel chromatography with chloroform : methanol=9 : 1 as eluent. The yield of H_2PFPP-C_2-H_2PFPP was 77% (310 mg).

^{1}H NMR ($CDCl_3$) $\delta=-2.9$ (4H, s, pyrrole-NH), 4.1 (4H, s, methylene), 8.1 (2H, s, amide N-H), 8.4 (8H, s, Ar), 8.9 (16H, m, pyrrole-β-H); UV (CH_2Cl_2–10%EtOH) λ_{max} 413 nm (ε 603 $mM^{-1}\,cm^{-1}$), 508 (41), 540 (6.82), 584.5 (13.5), 638 (2.86); Emission (CH_2Cl_2–10%EtOH) λ_{max} (Ex.=413 nm) 643 nm, 707.5; MS (FAB) m/z 1881 (MH^+).

H_2DCPP-C_2-H_2DCPP: This compound was prepared from H_2DCPPCOOH in a way like that described for the preparation of H_2PFPP-C_2-H_2PFPP. The yield was 89%. ^{1}H NMR ($CDCl_3$) $\delta=-2.6$ (4H, s, pyrrole-NH), 4.3 (4H, s, methylene), 7.5—7.6 (18H, m, 2,6-dichlorophenyl 3-H, 4H and 5-H), 7.7—7.8 (8H, m, carboxylphenyl), 8.7 (16H, m, pyrrole-β-H); UV (CH_2Cl_2–10%EtOH) λ_{max} 417.5 nm (ε 820 $mM^{-1}\,cm^{-1}$), 512 (41.5), 589 (15.2); MS (FAB) m/z 1754 (M).

H_2DCPP-C_2-H_2PFPP, H_2TTP-C_2-H_2PFPP, Mn-PFPP-C_2-H_2PFPP, and H_2TTP-C_2-H_2P(COOMe)$_3$. As one example, the synthesis of H_2DCPP-C_2-H_2PFPP will be described. H_2DCPPCOOH (200 mg, 0.231 mmol) was dissolved in dry benzene (20 ml); then and thionyl chloride (1.7 ml, 23.1 mmol) was added. The solution was brought to reflux for 1.5 h and the solvent was removed under reduced pressure. The acid chloride H_2PFPPPCOCl (0.231 mmol) was also prepared by the above method. The acid chloride H_2DCPPCOCl was redissolved in benzene (10 ml) and once again taken to dryness under reduced pressure to remove traces of thionyl chloride. The acid chloride was redissolved in $CHCl_3$ (30 ml) and this mixture was added dropwise to a liquid of ethylenediamine (690 mg, 11.6 mmol). The solution was brought to reflux for 1 h and then the reaction was quenched by addition of water. The $CHCl_3$ layer was then separated and dried over $MgSO_4$. The chloroform was removed under reduced pressure; next the residue was redissolved in $CHCl_3$ (30 ml), and H_2PFPPPCOCl was added. The resulting solution was brought to reflux for 1.5 h. The sample was purified by silica gel chromatography with chloroform : methanol=9 : 1 as eluent. The yield of H_2DCPP-C_2-H_2PFPP was 94% (369 mg).

H_2DCPP-C_2-H_2PFPP: The yield was 94%. ^{1}H NMR ($CDCl_3$) $\delta=-2.9$ (4H, s, pyrrole-NH), 4.1 (4H, s, methylene), 7.6—7.8 (11H, m, 2,6-dichlorophenyl 3-H, 4-H and 5H, and amide N-H), 8.3 (8H, s, Ar), 8.6—8.95 (16H, m, pyrrole-β-H); UV (CH_2Cl_2–10%EtOH) λ_{max} 416 nm (ε 645 $mM^{-1}\,cm^{-1}$), 511.5 (38.8), 540 (6.6), 588 (12.41), 644 (1.7); Emission (CH_2Cl_2–10%EtOH) λ_{max} (Ex.=416 nm) 645 nm, 707.5; MS (FAB) m/z 1818 (MH^+).

H_2TTP-C_2-H_2PFPP: The yield was 60.2%. ^{1}H NMR ($CDCl_3$) $\delta=-2.84$ (4H, s, pyrrole-NH), 3.94 (4H, bs, methylene), 7.7 (2H, s, amide N-H), 7.50 (6H, m, tolyl 3-H and 5-H), 8.08 (6H, m, tolyl 2-H and 6-H), 8.16—8.40 (8H, m, carbamoylphenyl), 8.68—9.54 (16H, m, pyrrole-β-H); UV (CH_2Cl_2–10%EtOH) λ_{max} 416 nm (ε 592 $mM^{-1}\,cm^{-1}$), 513 (32.1), 545.5 (8.75), 585.5 (11.7), 644.5 (2.92); Emission (CH_2Cl_2–10%EtOH) λ_{max} (Ex.=416 nm) 652 nm, 709.5; MS (FAB) 1654 (MH^+).

MnPFPP-C_2-H_2PFPP: The yield was 47%. UV ($CHCl_3$) λ_{max} 415 nm (ε 351.5 $mM^{-1}\,cm^{-1}$), 475 (121.4), 509 (28.31), 581 (17.41); MS (FAB) 1934 (MH^+).

H_2TTP-C_2-H_2P(COOMe)$_3$: The yield was 20%. ^{1}H NMR $\delta=-2.8$ (4H, d, pyrrole-NH), 2.63 (6H, s, Me), 2.7 (3H, s, Me), 4.05 (4H, bs, methylene), 4.08 (6H, s, ester-Me), 4.11 (3H, s, ester-Me), 7.45—8.12 (12H, m, Ar), 8.25—8.45 (20H, m, Ar), 7.62 (1H, t, amide), 7.78 (1H, t, amide), 8.76—8.90 (16H, m, pyrrole-β-H), UV (CH_2Cl_2–10%EtOH) λ_{max} 417 nm (ε 848 $mM^{-1}\,cm^{-1}$), 513 (38.4), 547 (20.7), 587 (14.4), 642 (10.5), MS (FAB) m/z 1558 (MH^+).

Zinc-Hybrid Porphyrin Dimer: ZnTTP-C_2-H_2PFPP, ZnTTP-C_2-H_2TTP, ZnPFPP-C_2-H_2PFPP, and ZnPFPP-C_2-H_2TTP. As one example, the synthesis of ZnTTP-C_2-H_2PFPP will be described. H_2TTPCOOH (40 mg 5.7×10^{-5} mol) and ethylenediamine (76 μl, 1.14×10^{-3} mol) was reacted by the above method (see H_2DCPP-C_2-H_2PFPP). The reaction was quenched by addition of water. The $CHCl_3$ layer was then separated and dried over anhydrous magnesium sulfate. The chloroform was removed under reduced pressure and the sample was purified by silica gel chromatography with chloroform : methanol=9 : 1 as eluent. H_2TTP-C_2-NH_2 was dissolved in $CHCl_3$ (10 ml), and zinc acetate dihydrate (125 mg, 5.7×10^{-4} M) in methanol (4 ml) was added. The resulting solution was brought to reflux for 1 h. The solution was washed by water (30 ml) to remove excess zinc salt; the $CHCl_3$ layer was then separated, and dried over magnesium sulfate. The chloroform was removed under reduced pressure. H_2PFPPPCOOH (52.9 mg, 5.7×10^{-5} mol) was reacted with $SOCl_2$ in a similar way to that described above. The acid chloride was dissolved in chloroform (5 ml) and this mixture was added to ZnTTP-C_2-NH_2 solution (chloroform, 5 ml) in the presence of 3 drops of triethylamine. The resulting solution was brought to reflux for 1 h. The sample was purified by silica gel chromatography with chloroform : acetone=9 : 1 as eluent. The yield of ZnTTP-C_2-H_2PFPP was 37% (36.2 mg).

ZnTTP-C_2-H_2PFPP: The yield was 37%. ^{1}H NMR $\delta=-2.99$ (2H, d, pyrrole-NH), 1.20 (4H, d, methylene), 2.50 (6H, s, Me), 2.65 (3H, s, Me), 7.7 (2H, bs, amide N-H), 7.35—8.30 (20H, m, Ar), 8.85—9.10 (16H, m, pyrrole-β-H); UV (CH_2Cl_2–10%EtOH) λ_{max} 430.5 nm (ε 1040 $mM^{-1}\,cm^{-1}$), 510 (36.1), 565 (36.1), 601 (20.6); MS (FAB) m/z 1717 (MH^+ for ^{64}Zn).

ZnTTP-C_2-H_2TTP: The yield was 44%. ^{1}H NMR $\delta=-2.8$ (2H, d, pyrrole-NH), 2.20 (4H, s, methylene), 2.15 (27H, s, tolyl), 5.35 (2H, bs, amide), 7.6 (12H, d, tolylphenyl 3-H and 5-H), 8.10 (12H, d, tolyl 2-H and 6-H), 8.30 (4, d, carbamoylphenyl 3-H and 5-H), 8.50 (4, d, carbonylphenyl 2-H and 6-H), 8.70—9.00 (16H, m, pyrrole-β-H); UV (CH_2Cl_2–10%EtOH) λ_{max} 429.5 nm (ε 829 $mM^{-1}\,cm^{-1}$),

514.5 (29.3), 556.5 (33.5), 603.5 (20.9), 646 (8.38); MS (FAB) m/z 1488 (M for ^{64}Zn).

ZnPFPP-C_2-H_2TTP: ^{1}H NMR $\delta=-2.70$ (2H, d, pyrrole-NH), 1.23 (4H, d, methylene), 2.25 (6H, s, tolyl), 2.75 (3H, s, tolyl), 7.60—8.55 (22H, m, aromatic, amide), 8.85—9.10 (16H, m, pyrrole-β-H); UV (CH_2Cl_2–10%EtOH) λ_{max} 422 nm (ε 490 $mM^{-1}\,cm^{-1}$), 515 (14.9), 554 (27.0), 594 (11.4), 645 (2.28); MS (FAB) m/z 1716 (MH^+ for ^{64}Zn).

ZnPFPP-C_2-H_2PFPP: ^{1}H NMR $\delta=-3.05$ (2H, d, pyrrole-NH), 3.60 (4H, bs, CH_2), 6.25 (2H, bs, amide-NH), 7.73 (4H, d, Zn-aromatic 3-H and 5H), 8.05 (4H, d, Zn-aromatic 2-H and 6-H), 8.65—8.95 (20H, m, pyrrole-β-H and free base-Ar 2-H, 3-H, 5-H and 6-H); UV (CH_2Cl_2–10%EtOH) λ_{max} 426 nm (ε 799 $mM^{-1}\,cm^{-1}$), 511 (33.6), 557 (33.6), 583.5 (16.8); MS (FAB) m/z 1944 (MH^+ for ^{64}Zn).

ZnPFPPCOOMe: UV (benzene–1% pyridine) λ_{max} 426.5 nm, 555; Emission (benzene–1% pyridine) λ_{max} (Ex.= 430.5) λ_{max} 614.5 nm, 664.

Manganese(III) Complexes of Porphyrins: MnPFPP-C_2-MnPFPP, MnPFPP-C_2-MnDCPP, MnDCPP-C_2-MnDCPP, MnPFPP, MnPFPPCOOMe, MnPFPPCOOH, MnDCPP, MnDCPPCOOMe, and MnTTP-C_2-MnP(COOMe)$_3$. As one example, the synthesis of MnPFPP-C_2-MnPFPP will be described. First 510 mg of H_2PFPP-C_2-H_2PFPP (0.28 mmol) and 510 mg of bis(2,4-pentanedionato) manganese(II) (2.8 mmol) were dissolved in DMI (1,3-dimethyl-2-imidazolidinone, 14 ml). The solution was brought to reflux for 30 min. and the solvent was removed under reduced pressure. When distilled water (10 ml) was added, black precipitates appeared. These precipitates were filtrated by membrane filter (ADVANTEC, pore size 0.5 μm) and redissolved in chloroform, and then dried over $MgSO_4$. The solvent was removed under reduced pressure. The sample was purified by alumina chromatography with chloroform : methanol=4 : 1 as eluent. The yield was 30% (90 mg).

UV λ_{max} ($CHCl_3$) 473 nm (ε 62 $mM^{-1}\,cm^{-1}$), 572 (8.95); MS (FAB) m/z 1988 (MH^+).

MnPFPP-C_2-MnDCPP: UV ($CHCl_3$) λ_{max} 474.5 nm (ε 142 $mM^{-1}\,cm^{-1}$), 573.5 (19.9); MS (FAB) m/z 1924 (MH^+).

MnDCPP-C_2-MnDCPP: UV ($CHCl_3$) λ_{max} 477 nm (ε 173.9 $mM^{-1}\,cm^{-1}$), 579 (19.7); MS (FAB) m/z 1860 (M).

MnPFPP: UV ($CHCl_3$) λ_{max} 473 nm (ε 52.8 $mM^{-1}\,cm^{-1}$), 572 (6.90); MS (FAB) m/z 1027 (M).

MnPFPPCOOMe: UV ($CHCl_3$) λ_{max} 474 nm (ε 91.6 $mM^{-1}\,cm^{-1}$), 573 (10.8).

MnPFPPCOOH: UV ($CHCl_3$) λ_{max} 468.5 nm, 569.5; MS (FAB) m/z 981 (M).

MnDCPP: UV ($CHCl_3$) λ_{max} 476 nm (ε 77.7 $mM^{-1}\,cm^{-1}$), 574 (6.27); MS (FAB) m/z 943 (M).

MnDCPPCOOMe: UV ($CHCl_3$) λ_{max} 475.5 nm (ε 116 $mM^{-1}\,cm^{-1}$), 561.5 (13.3).

MnTTP-C_2-MnP(COOMe)$_3$: This compound was prepared by using $CHCl_3$/pyridine as described previously.[1] UV ($CHCl_3$) λ_{max} 468 nm (ε 98.5 $mM^{-1}\,cm^{-1}$), 568 (13.2), 605 (10.8).

Measurements. Nuclear Magnetic Resonance Spectra: NMR spectra were taken with a Varian Gemini 300 instrument, operating at 300 MHz. Tetramethylsilane was used as internal standard.

UV-vis Spectra: Absorption spectra were taken with a Hitachi 124 recording spectrophotometer at 25 °C. Solutions were prepared in $CHCl_3$ and egg yolk PC liposome in 0.4 M imidazole buffer (pH 7.0).

Steady State Fluorescence Spectra: Steady state fluorescence spectra were taken with a JASCO FP-777 recording spectrophotometer at 25 °C. Solutions were prepared in $CHCl_3$ and egg yolk PC liposome in 0.1 M bis–tris buffer (pH 7.0). The absorbance of the sample solution was set at 0.2.

Cyclic Voltammetry: Each cyclic voltammogram was taken on a Yanako P-900 with SCE as reference electrode, glassy carbon as working electrode, and platinum as counter electrode. The samples were prepared in DMSO containing 0.1 M tetrabutylammonium perchlorate (TBAP) at a concentration of 3×10^{-4} mol dm^{-3}. The solutions were degassed by argon bubbling.

Mass(FAB) Spectroscopy: Mass spectroscopy was performed on a JEOL JMS-SX 102A with m-nitrobenzyl-alcohol as matrix.

Preparation of Egg PC Liposome Containing Manganese(III) Porphyrin Dimers for Transmembrane Electron Transfer Assay. Liposomes containing manganese porphyrin dimers were prepared by previously reported methods for incorporating metalloporphyrins into egg yolk phosphatidylcholine (PC) liposomes.[1,14] Egg yolk phosphatidylcholine (100 mg, a gift from Nippon Fine Chemical Co.) was dissolved in one milliliter of $CHCl_3$. Desired manganese porphyrin dimers in $CHCl_3$ were added, and mixed together, and the solvent was removed on a rotary evaporator. The porphyrin–lipid film was suspended in 2.5 ml of 0.1 M $K_3Fe(CN)_6$ in 0.4 M imidazole buffer, pH 7.0, by gentle swirling. The smooth, turbid suspension was sonicated at 0 °C under a stream of nitrogen by using a Branson Model 250 Sonifier for 10 min. The vesicle samples were then subjected to a Sephadex G-25-80 gel filtration column (1.5 cm i.d.×15 cm long) using 0.025 M KCl and 0.175 M NaCl in 0.4 M imidazole, pH 7.0, as the eleuting buffer. The fraction containing the liposome was collected with little dilution. Oxygen was removed from the vesicles by passing argon gas over and through the liposome solution for about 30 min. The liposomes were then stored under inert gas until needed for the electron transfer assay, which was performed the same day.

Transmembrane Electron Transfer Assay. Transmembrane electron transport from an external reductant, indigotetrasulfonic acid ($ITSAH_2$, 1.0×10^{-4} M) reduced by $Na_2S_2O_4$ (1.0×10^{-4} M), to hexacyanoferrate (III) (0.1 M) trapped within an egg phosphatidylcholine (PC) liposome, as mediated by a catalyst incorporated in the lipid bilayer, was studied by monitoring the appearance of oxidized indigotetrasulfonic acid (ITSA, $\lambda_{max}\approx605$ nm). Conditions for this assay were nearly identical with those previously published.[1,14]

Results and Discussion

The Synthesis of Porphyrin Dimers. MnPFPP-C_2-H_2PFPP, ZnTTP-C_2-H_2PFPP, ZnTTP-C_2-H_2TTP, ZnPFPP-C_2-TTP, and ZnPFPP-C_2-PFPP were prepared as outlined in Scheme 3. H_2PFPP-C_2-H_2PFPP, H_2DCPP-C_2-H_2DCPP, H_2DCPP-C_2-H_2PFPP, H_2TTP-

C_2-$H_2P(COOMe)_3$, and their manganese(III) complexes were prepared as outlined in Scheme 4. The porphyrin dimers were covalently linked via two amide linkage to ethylenediamine, because the ethylene bridge is flexible and the amide bonds are chemically stable. Thus, the porphyrin dimers are likely to take on proper conformation by perturbation the lipid bilayers of liposomal membrane. The porphyrin derivatives, H_2PFPPCOOMe and H_2DCPPCOOMe (Scheme 2), were synthesized by the porphyrin condensation reaction with halogenated benzaldehyde, p-methoxycarbonylbenzaldehyde, and pyrrole in CH_2Cl_2 in the presence of diethyl ether–boron trifluoride (1/1) according to a useful method reported previously.[13] H_2TTPCOOMe

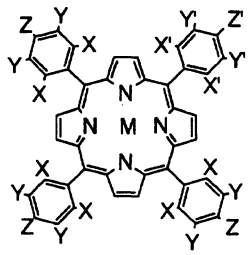

	M	X	Y	Z	X'	Y'	Z'
H_2PFPP	H_2	F	F	F	F	F	F
H_2PFPPCOOMe	H_2	F	F	F	H	H	COOMe
ZnPFPPCOOMe	Zn	F	F	F	H	H	COOMe
MnPFPP	Mn	F	F	F	F	F	F
MnPFPPCOOMe	Mn	F	F	F	H	H	COOMe
H_2DCPP	H_2	Cl	H	H	Cl	H	H
H_2DCPPCOOMe	H_2	Cl	H	H	H	H	COOMe
MnDCPPCOOMe	Mn	Cl	H	H	H	H	COOMe
H_2TTP	H_2	H	H	Me	H	H	Me
H_2TTPCOOMe	H_2	H	H	Me	H	H	COOMe
ZnTTPCOOMe	Zn	H	H	Me	H	H	COOMe
MnTTP	Mn	H	H	Me	H	H	Me
$H_2P(COOMe)_3COOH$	H_2	H	H	COOMe	H	H	COOH

Scheme 2. Halogenated porphyrin monomers.

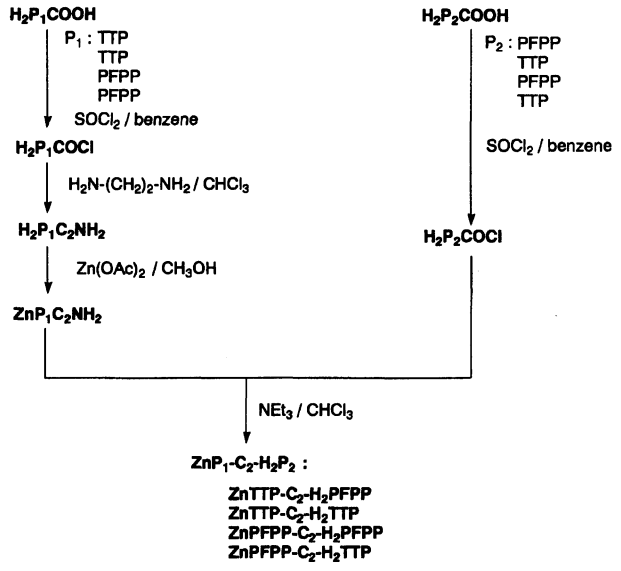

Scheme 3. Outline of synthetic methods of zinc hybrid porphyrin dimers.

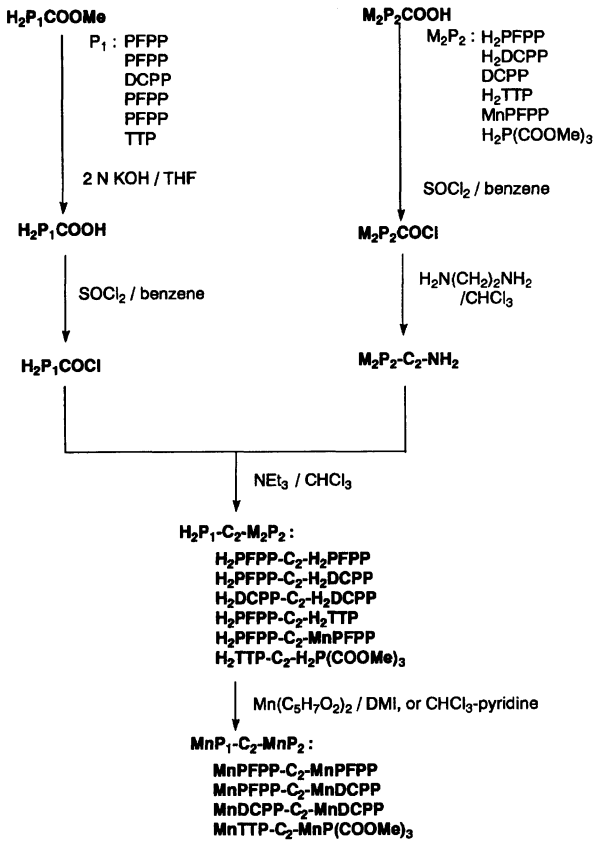

Scheme 4. Outline of synthetic methods of manganese halogenated porphyrin dimers.

and $H_2P(COOMe)_3COOH$ (Scheme 2) were also synthesized by the porphyrin condensation reaction with *p*-methylbenzaldehyde, *p*-methoxycarbonylbenzaldehyde, and pyrrole in propionic acid according to a useful method reported previously.[1,12] The (*p*-carboxyphenyl)porphyrins were then obtained by base-catalyzed hydrolysis of the (*p*-methoxycarbonylphenyl)porphyrins and subsequent acidification. In Schemes 3 and 4, to introduce ethylene chain between porphyrins, the (*p*-carboxyphenyl)porphyrins were converted to the acid chlorides by reaction with thionyl chloride, followed by reaction with ethylenediamine to give the porphyrin dimer. Zinc complexes of porphyrins were prepared via treatment with zinc acetate. The manganese complexes of porphyrin dimers were prepared by reaction with bis(2,4-pentanedionato)manganese(II). Manganese insertion reaction was carried out in 1,3-dimethyl-2-imidazolidinone at 160 °C. The manganese insertion into halogenated free-base porphyrin gave low yield (about 10%), while the yield of manganese insertion into H_2TTP-C_2-$H_2P(COOMe)_3$ is about 30%. These results imply that the steric hindrance of the halogen groups and also the electron deficient halogen moiety on the porphyrin ring inhibit manganese insertion into the porphyrin ring. The resulting porphyrin dimers were purified by silica gel column chromatography. The characterization and verification of the structures were done

by means of ^{1}H NMR, UV-vis spectra, and Mass spectroscopy (FABMASS), as described in the experimental section.

Redox Potential of Halogenated Porphyrin Derivatives. Redox potentials ($E_{1/2}$) of halogenated porphyrin derivatives were measured by cyclic voltammetry (CV) vs. SCE in DMSO–TBAP. Table 1 summarizes the redox potentials of MnPFPP-C_2-MnDCPP, MnDCPP-C_2-MnDCPP, MnPFPP-C_2-MnPFPP, and MnTTP-C_2-MnP(COOMe)$_3$. As is apparent from Table 1, the potential of Mn(II)/Mn(III) on glassy carbon electrode vs. SCE in DMSO–TBAP for the manganese complex follows the order: MnPFPP-C_2-MnPFPP (−0.10 V) > MnPFPP-C_2-MnDCPP (−0.18) > MnDCPP-C_2-MnDCPP (−0.21) > MnTTP-C_2-MnP(COOMe)$_3$ (−0.21). The redox potential decreases with decreasing of the halogen portions on the porphyrin ring, suggesting that the porphyrins become electrondeficient due to the presence of halogenated phenyl groups which withdraw electrons from the porphyrin ring.[15] Similar results were observed for halogenated porphyrin monomers. Interestingly, the redox potential of the manganese complex for MnPFPP-C_2-MnPFPP decreased with increasing of imidazole concentration (see Table 1), indicating that ligated imidazole tends to make the potential more negative. This result is consistent with the induced blue-shift of the Soret bands of manganese halogenated dimers due to addition of imidazole, as described below (see Fig. 1b).

UV-vis Spectra of Porphyrin Dimers in Dichloromethane and Liposomal Membrane. The UV-vis spectrum of H_2TTP-C_2-H_2PFPP in dichloromethane, for example, had λ_{max} at 416 (the Soret band), 513, 545.5, 585.5, and 644.5 nm, where the absorption spectrum was similar to a linear combination of those of H_2TTP and H_2PFPP. Similar results were also obtained for other porphyrin dimers, as described in the experimental section. These results indicate that no overlap of these molecular orbitals between porphyrin faces and/or edges in ground state occurs. Furthermore, the absorbance spectrum of H_2TTP-C_2-H_2PFPP in egg PC liposomal membrane was nearly identical with that in dichloromethane. Similar results were also obtained for all other porphyrin dimers, indicating that the porphyrin dimers are located in the hydrophobic environment of the liposomal membrane rather than in aqueous environment. The liposomal membrane containing 2 or 3 porphyrin dimers did not precipitate for 24 h, suggesting that the porphyrins are fairly stable in the lipid bilayers.

Figure 1 shows UV-vis spectra of MnPFPP-C_2-MnPFPP in chloroform in the absence and presence of imidazole, and in egg PC liposomal membrane. As in apparent from Fig. 1a, the UV-vis spectrum in the liposomal membrane is very similar to that in chloroform. Similar results were obtained for other manganese porphyrin dimers. These results again indicated that manganese halogenated porphyrin dimers are located in the hydrophobic environment of the liposomal membrane. As is apparent from Fig. 1b, the Soret band is located at 474 nm in chloroform when imidazole is not present, while the band is shifted to 460 nm when imidazole is present, indicating that imidazole binds to the manganese complexes of the porphyrins. The intensity of this band increases with increasing of imidazole concentration. From these spectral changes the equilibrium binding constant was determined to be 195 M^{-1}. Similar blue shifts were observed for other manganese halogenated porphyrin dimers. That is, the Soret bands of MnPFPP-C_2-MnDCPP, MnDCPP-C_2-MnDCPP, and MnPFPP-C_2-H_2PFPP were located at 475, 477, and 475 nm, respectively, when imidazole was not present, and the bands were shifted to 462, 465, and 461 nm, respectively, when imidazole is present. These results imply that imidazole is likely to work as an axial ligand of manganese halogenated porphyrin dimers in both lipid bilayers and chloroform. However, such a blue shift of the Soret band was not observed for MnTTP-C_2-MnP(COOMe)$_3$.

Fluorescence Emission Spectra of Halogenated Porphyrin Dimers in Dichloromethane and Egg PC Liposomal Membrane. Fluorescence spectra of halogenated porphyrin dimers in dichloromethane and egg PC liposomal membrane were measured to gain more information on these excited states and on the environment of halogenated porphyrin dimers in lipid bilayers.

Table 2 summarizes the emission maxima of free base and zinc hybrid dimers. Free base porphyrin dimers such as H_2TTP-C_2-H_2PFPP and H_2PFPP-C_2-H_2PFPP have two emission maxima in egg PC liposomal membrane and dichloromethane, while the zinc hybrid porphyrin dimers have three emission maxima. These fluorescence intensities are similar in both media. Thus, the data imply again that in the PC vesicle systems the porphyrin dimers are not located at the surface in an aqueous environment, but rather are immersed within the hydrophobic interior of the membrane.

Energy Transfer of Zinc Hybrid Dimers, ZnTTP-C_2-H_2PFPP, ZnTTP-C_2-H_2TTP, ZnPFPP-C_2-H_2PFPP, and ZnPFPP-C_2-H_2TTP. Zinc monomer porphyrins, ZnTTPCOOMe and ZnPFPPCOOMe have maxima at 615/664 and 604/655.5 nm, respectively. Free base monomer porphyrins, H_2PFPPCOOMe and H_2TTPCOOMe, have maxima at 643/707 nm and 654.5/717.5 nm, respectively. The fluorescence spectra of the zinc hybrid dimers are clearly a combination of these two monomer emission as shown in Table 2. However, in ZnTTP-C_2-H_2TTP and ZnPFPP-C_2-H_2TTP, emission from the zinc porphyrin moiety is strongly quenched in the dimers, relative to their mixed monomers, as shown in Fig. 2. Similar results were obtained for ZnTTP-C_2-H_2PFPP and ZnPFPP-C_2-H_2PFPP (the data are not shown). As is appar-

Table 1. Redox Potential (V) vs. SCE of Porphyrin Derivatives in DMSO Containing 0.1 M TBAP

Porphyrins	Redox potential[a]/V vs. SCE			
	Mn(II)/Mn(III)	Porphyrin ring		
MnPFPP-C_2-MnPFPP	−0.10	−1.01		−1.50
	(−0.15)[b]			
	(−0.16)[c]			
MnPFPP-C_2-MnDCPP	−0.18		−1.22 −1.37	−1.51
MnDCPP-C_2-MnDCPP	−0.21		−1.21	
MnTTP-C_2-MnP(COOMe)$_3$	−0.21		−1.15 −1.28	−1.57
MnPFPPCOOMe	−0.08	−0.95		−1.48
MnPFPP	−0.07	−0.95		−1.43
MnDCPPCOOMe	−0.17		−1.20	
MnDCPP	−0.18	−1.21		
MnTTP	−0.25	−1.29		
H_2PFPP		−0.71		−1.50
H_2TTP		−1.08		−1.54

a) The concentration was 3×10^{-4} M. The scan rate was 50 mV s^{-1}. b) In the presence of imidazole. The concentration was 0.88 M. c) In the presence of imidazole. The concentration was 1.80 M.

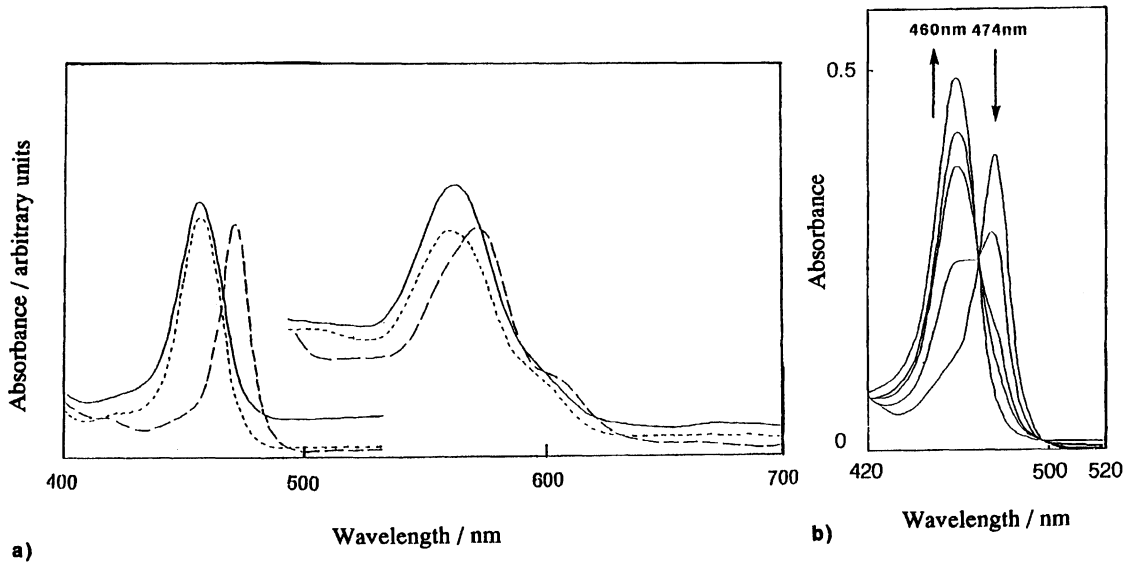

Fig. 1. a) UV-vis spectra of MnPFPP-C_2-MnPFPP. (---): in $CHCl_3$ in the absence of imidazole, (····): in $CHCl_3$ in the presence of imidazole, (—): in egg PC liposomal membrane at pH 7.0, 0.4 M imidazole buffer. b) UV-vis spectra (Soret region) of MnPFPP-C_2-MnPFPP in the various concentrations of imidazole. The imidazole concentrations were 0, 0.6, 1.5, 2.5, and 3.5 mM. The concentration of manganese porphyrin was 10 μM.

ent from Fig. 2, if one compares the emission spectra for the mixed monomers and Zn hybrid dimers due to excitation for ZnTTP at 429 nm or ZnPFPP at 426 nm, one sees that 85.4 or 85.3% quenching of zinc porphyrin fluorescence was observed in ZnTTP-C_2-H_2TTP or ZnPFPP-C_2-H_2TTP. Also, 82.2 or 76.8% quenching of zinc porphyrin fluorescence in ZnTTP-C_2-H_2PFPP or ZnPFPP-C_2-H_2PFPP was observed (the data are not shown). Correspondingly, if one compares the emission band due to the free base monomers in the mixed monomer systems with the same band in the Zn hybrid dimer system as caused once again by excitation at 429 nm or 420 nm, it is apparent that there is a substantial increase in the fluorescence intensity of the free base porphyrin at 725 nm for both ZnTTP-C_2-H_2TTP and ZnPFPP-C_2-H_2TTP, and also at 711 nm for both ZnTTP-C_2-H_2PFPP and ZnPFPP-C_2-H_2PFPP (the data are not shown). Since the concentration of the porphyrin solutions is low, the change in these fluorescence intensities is likely due to an intramolecular quenching of the zinc porphyrin moiety by free base porphyrin moiety. Preliminary studies on a Zinc hybrid dimer, ZnTTP-C_n-H_2TTP (n=2, 3) and one porphyrin-linked quinone with various carbon lengths (C_n, n=2, 3, 4, 6) indicated that more efficient energy transfer or electron transfer occurred only when n=2 or 3.[4,6,16,17] Thus,

Table 2. The Steady State Fluorescence Emission Wavelength for Halogenated Porphyrin Dimers in Organic Solvent and Egg PC Liposome

Porphyrins	Medium	Emission maxima[a]/nm		
H_2PFPP-C_2-H_2PFPP	CH_2Cl_2[b]		643	707.5
	egg PC liposome		645	709
H_2PFPP-C_2-H_2TTP	CH_2Cl_2[b]		652	709.5
	egg PC liposome		654	712
H_2PFPPCOOMe	CH_2Cl_2[b]		643	707
H_2TTPCOOMe	CH_2Cl_2[b]		654.5	717.5
ZnTTP-C_2-H_2PFPP	benzene[c]	615.5	646.5	710.5
	egg PC liposome	610.5	647.0	709.5
ZnTTP-C_2-H_2TTP	benzene[c]	614.5	654.5	718
	egg PC liposome	611.0	654.5	718
ZnPFPP-C_2-H_2PFPP	benzene[c]	605.5	647.5	710.5
	egg PC liposome	605.5	647	709.5
ZnPFPP-C_2-H_2TTP	benzene[c]	605.5[d]	654.5	718
	egg PC liposome	605.5[d]	654.5	718
ZnPFPPCOOMe	benzene[c]	604	655.5	
ZnTTPCOOMe	benzene[c]	615	664	

a) Solutions of the porphyrin derivatives were adjusted to have equal absorbances of 0.20 at the Soret band λ_{max}. b) Including 10% EtOH. c) Including 1% pyridine. d) Shoulder.

linking the porphyrins with an ethylenediamine moiety has opened up new pathways for decay of both excited singlet states. However, no or less fluoresecence quenching was observed between porphyrins for free base porphyrin dimers, H_2PFPP-C_2-H_2TTP and H_2PFPP-C_2-H_2PFPP.

The most probable mechanism for the observed energy transfer is the Forster dipole–dipole interaction. A value for the quantum efficiency of the energy transfer (Φ_{et}) for ZnTTP-C_2-H_2PFPP, ZnTTP-C_2-H_2TTP, ZnPFPP-C_2-H_2TTP, and ZnPFPP-C_2-H_2PFPP may be calculated using the following equation[6,18]

$$\Phi_{et} = 1 - I_H/I_0,$$

where I_H is the fluorescence intensity of a dimer; and I_0 is that of ZnTTPCOOMe and ZnPFPPCOOMe at 615 nm, respectively.

Values of the quantum efficiency of the energy transfer (Φ_{et}) were obtained using the equation (Table 3). From the data presented in Table 3, light absorbed by Zn porphyrin of the porphyrin dimers is very efficiently transferred to the free base porphyrin and is emitted from that center with a quantum yield which must be near that of the free base monomer. However, less Φ_{et} were observed for ZnTTP-C_2-H_2PFPP in comparison to the results for ZnTTP-C_2-H_2TTP. Furthermore, Φ_{et} for ZnPFPP-C_2-H_2PFPP decreased in comparison with that for ZnPFPP-C_2-H_2TTP. Thus, the energy transfer in the zinc hybrid dimers is likely to depend on the structure and redox potential of the acceptor porphyrins. More detailed kinetic study will be reported elsewhere.

Table 3. The Quantum Efficiency (Φ_{et}) of the Energy Transfer

Porphyrins	Φ_{et}[a]
ZnTTP-C_2-H_2PFPP	0.822
ZnTTP-C_2H_2TTP	0.854
ZnPFPP-C_2-H_2PFPP	0.768
ZnPFPP-C_2-H_2TTP	0.853

a) $\Phi_{et} = 1 - I_H/I_0$. I_H is the fluorescence intensity of dimer at 615 nm and I_0 is that of ZnTTPCOOMe and ZnPFPPCOOMe at 615 nm, respectively.

Transmembrane Electron Transfer Catalyzed by Manganese(III) Halogenated Porphyrin Dimers. The manganese(III) complexes of porphyrin dimers were incorporated in a standard electron transport assay system to study its catalytic activity of transmembrane electron transfer at pH=7.0. Electron transfer from an external reductant (reduced indigotetrasulfonic acid, $ITSAH_2$, 1×10^{-5} M) to internal potassium hexacyanoferrate(III) (0.1 M) trapped within an egg yolk phospholipid liposome (egg PC) was measured anaerobically at 0.4 M imidazole buffer as mediated by a catalyst of manganese porphyrin derivatives incorporated in the vesicle bilayer.[1,14] The oxidized form of the dye, ITSA, has an intense absorbance band at $\lambda_{max}=600$ nm. The intensity and positions of this band permitted us to measure the rate of the electron transfer with minimal spectroscopic interference from the other components of the model system. The initial electron transfer rate (V_0) was determined from the initial slope of the change of absorption band at 600 nm. Figure 3 illustrates the rate of electron transport across egg PC liposomes (V_0). As is apparent from this figure, manganese(III) halogenated porphyrin dimers showed

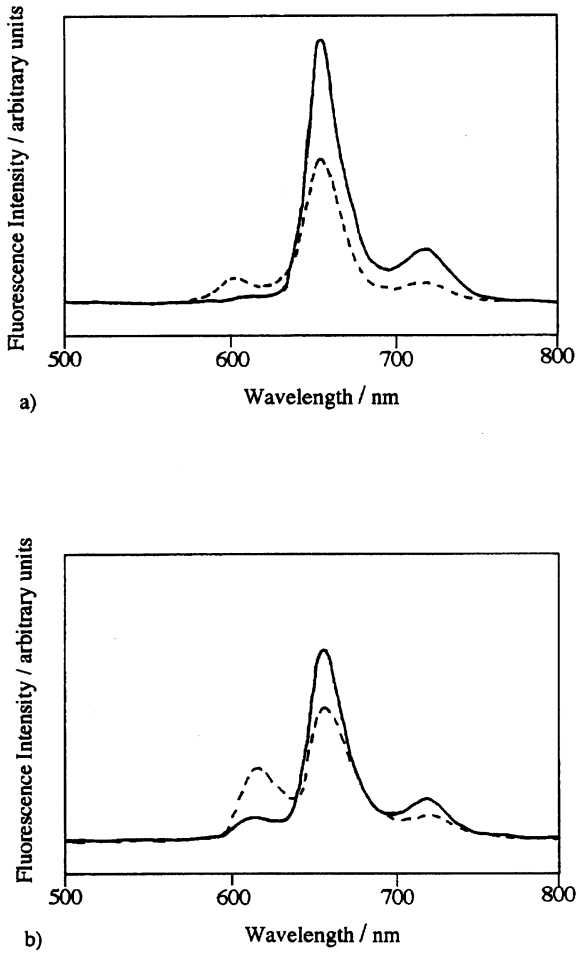

Fig. 2. The fluorescence emission spectra (uncorrected). a) ZnPFPP-C_2-H_2TTP (solid line) and mixed monomers, ZnPFPPCOOMe and H_2TTPCOOMe (dashed line) in benzene–1% pyridine. Excitation wavelength was 426 nm. b) ZnTTP-C_2-H_2TTP (solid line) and mixed monomers, ZnTTPCOOMe and H_2TTPCOOMe (dashed line) in benzene–1% pyridine. Excitation wavelength was 429 nm. The Zn hybrid dimer and mixed monomers, Zn monomer and free base monomer solutions were 0.20 O.D. at the maximum of absorbance in the Soret region.

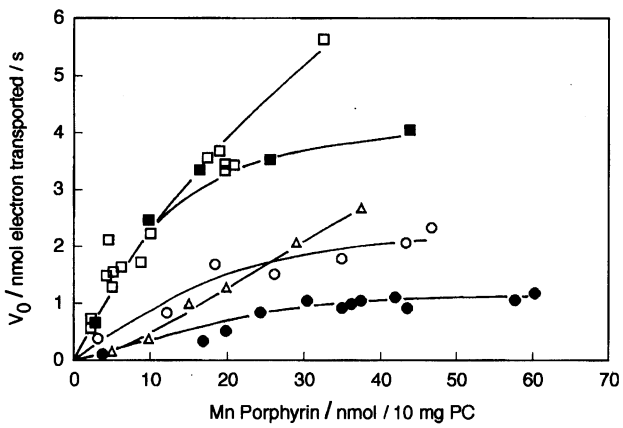

Fig. 3. Dependence of the rate of electron transport by manganese halogenated porphyrin dimers with reductants. The X-axis expresses the quantity of metalloporphyrin in 10 mg of egg york phosphatidylcholine at 25 °C, anaerobic condition. (●): MnPFPP-C_2-MnPFPP, (○): MnPFPP-C_2-MnDCPP, (■): MnDCPP-C_2-MnDCPP, (□): MnTTP-C_2-MnP(COOMe)$_3$, (△): MnTTP.

catalytic activity with increasing the porphyrin concentration in the lipid bilayer. No or less electron transfer was observed when imidazole was not present and also when free base porphyrin dimers such as H_2TTP-C_2-H_2P(COOMe)$_3$ were used (the data are not shown).

The mechanism of electron transfer is presumed to follow a pathway as illustrated below.[1,14] Electron transfer occurs from external reduced indigotetrasulfonic acid to an oxidized manganese porphyrin. The semiquinone form of indigotetrasulfonic acid would be expected to disproportionate rapidly in water. The reduced manganese porphyrin is then diffused to the inner half of the lipid bilayer contacted with hexacyanoferrate(III) ions. The electron transfer to hexacyanoferrate(III) is then completed by movement of the manganese(II) porphyrin on the inner half of the bilayer where it can donate an electron to a hexacyanoferrate(III) molecule. In analogy to previous studies with iron protoporphyrin IX dimethylester and manganese tetratolylporphyrins, where the rate-limiting step was the reaction with $ITSAH_2$.[1,14] We assume that diffusion in a transverse direction (perpendicular to the membrane plane) is fast relative to electron-transfer reactions. Furthermore, at the concentrations employed, electron transfer at the hexacyanoferrate(III) interface is assumed to be faster than that at $ITSAH_2$ interface. Thus, the electron transfer rate depends upon the oxidation of $ITSAH_2$ by manganese porphyrins in the outer phase of the lipid bilayers, where it is considered in analogy to our previous kinetic studies with MnTTP and MnPFPP that a stereospecific interaction of manganese porphyrins with the $ITSAH_2$ plays a more important role on the electron transfer than the order of the potential for the Mn(II)/Mn(III) (see Table 1) to oxidize $ITSAH_2$ on the outer phase of the lipid bilayers.[19] As is apparent from Fig. 3, the electron transfer rate decreased in the order, MnTTP-C_2-MnP(COOMe)$_3$ > MnDCPP-C_2-MnDCPP > MnDCPP-C_2-MnPFPP > MnPFPP-C_2-MnPFPP, which is not in agreement with the order of the potential for the Mn(II)/Mn(III) (see Table 1) to oxidize $ITSAH_2$ on the outer phase of the lipid bilayers. This result also indicates that the electron transfer catalyzed by manganese porphyrin dimers is likely to depend on the steric effect of halogen portions on the porphyrin dimers rather than on the oxidation potentials of the porphyrin dimers to oxidize $ITSAH_2$. Interestingly, an enhanced rate was observed for MnTTP-C_2-MnP(COOMe)$_3$ in comparison to that for MnTTP at this condition, as shown in

Fig. 3, implying that the manganese dimer has a crucial effect on the electron transfer. Furthermore, in the previous paper,[4,16] the result of transmembrane electron transfer catalyzed by MnTTP-C_n-MnP(COOMe)$_3$ (n=2, 3, 4, 6, 12) showed that the electron transfer depended on the length of methylene groups between the porphyrin dimer, in which an enhanced rate was observed only when n=2 or 3. These results indicated that an intramolecular electron transfer between porphyrins is likely to play also an important role on the electron transfer reaction. More detailed kinetics will be reported elsewhere.

In conclusion, Zn hybrid porphyrin dimers and manganese(III) halogenated porphyrin dimers (Scheme 1) were synthesized. These porphyrin dimers were stable in the lipid bilayers of liposomal membrane and also against oxidant, exhibiting unique reactivities because of the steric and electron-withdrawing effects of halogen portions on the porphyrin ring. An efficient energy transfer of the excited singlet state in the covalently-linked zinc hybrid dimers from zinc porphyrin to a free base porphyrin was observed, depending on the porphyrin structure. Furthermore, the manganese porphyrin dimers acted as catalysts of transmembrane electron transfer, revealing that the catalytic activity depends on the steric effect of halogen portions on the porphyrin rings. Thus, appropriate analogs of these halogenated porphyrin dimers are being utilized to systematically examine photochemical and catalytic activities in selected lipid bilayer systems. Results of these detailed studies will be reported elsewhere.

Thanks are due to the Instrument Center, the Institute for Molecular Science and Dr. Junji Yoshinaga, Sawai Pharmaceutical Co., Ltd. for assistance in determining the Mass (FAB) spectra. The present work was partially supported by a Grand-in-Aid No. 05680500 from the Ministry of Education, Science and Culture.

References

1) M. Nango, T. Dannhauser, D. Huang, K. Spears, L. Morrison, and P. A. Loach, *Macromolecules*, **17**, 1898 (1984); T. Dannhauser, M. Nango, N. Oku, K. Anzai, and P. Loach, *J. Am. Chem. Soc.*, **108**, 5865 (1986); M. Nango, A. Mizusawa, T. Miyake, and J. Yoshinaga, *J. Am. Chem. Soc.*, **112**, 1640 (1990).

2) M. Nango, K. Iida, T. Kawakita, M. Matsuura, Y. Harada, K. Yamashita, K. Tsuda, and Y. Kimura, *J. Chem. Soc., Chem. Commun.*, **1992**, 545.

3) K. Iida, M. Nango, K. Okada, S. Matsumoto, M. Matsuura, K. Yamashita, K. Tsuda, Y. Kurono, and Y. Kimura, *Chem. Lett.*, **1994**, 1307.

4) K. Iida, M. Nango, M. Hikita, T. Tajima, T. Kurihara, K. Yamashita, K. Tsuda, T. Dewa, J. Komiyama, M. Nakata, and Y. Ohtsuka, *Chem. Lett.*, **1994**, 1157.

5) "Photosynthesis," ed by Govinjee, Academic Press, New York (1982); "The Photosynthetic Bacteria," ed by R. K. Clayton and W. R. Sistrom, New York (1978); "Topics in Photosynthesis," ed by J. Barber, Elsevier/North-Holland Biochemical Press, New York (1979); J. Deisenhofer, O. Epp, K. Miki, R. Huber, and H. Michel, *Nature*, **318**, 618 (1985); W. A. Cramer and D. B. Knaff, "Energy Transduction in Biological Membranes," Springer-Verlag, New York (1991).

6) J. Anton, P. A. Loach, and Govindjee, *Photochem. Photobiol.*, **28**, 235 (1978).

7) D. Gust, T. A. Moore, A. L. Moore, L. Leggett, S. Lin, J. M. Degraziano, R. M. Hermant, D. Nicodem, P. Craig, G. R. Seely, and R. A. Nieman, *J. Phys. Chem.*, **97**, 7926 (1993).

8) A. Osuka, K. Maruyama, N. Mataga, T. Asahi, I. Yamazaki, and N. Tamai, *J. Am. Chem. Soc.*, **112**, 4958 (1990); A. Helms, D. Heiler, and G. McLendon, *J. Am. Chem. Soc.*, **114**, 6227 (1992).

9) A. Osuka, F. Kobayashi, S. Nakajima, K. Maruyama, I. Yamazaki, and Y. Nishimura, *Chem. Lett.*, **1993**, 161.

10) P. R. Ortiz de Montellano, "Cytochrome P-450, Structure, Mechanism and Biochemistry," Plenum Press, New York and London (1986).

11) S. Banfi, F. Legramandi, F. Mantanari, G. Pozzi, and S. Quici, *J. Chem. Soc., Chem. Commun.*, **1991**, 1285; J. F. Bartoli, O. Brigaud, P. Battioni, and D. Mansuy, *J. Chem. Soc., Chem. Commun.*, **1991**, 440; A. Sorokin, A. Robert, and B. Meunier, *J. Am. Chem. Soc.*, **115**, 7293 (1993); R. D. Arasasingham, G. -X. He, and T. C. Bruice, *J. Am. Chem. Soc.*, **115**, 7985 (1993); K. Miki and Y. Sato, *Bull. Chem. Soc. Jpn.*, **66**, 2385 (1993).

12) J. A. Anton and P. A. Loach, *J. Heterocycl. Chem.*, **12**, 573 (1975); J. A. Anton, J. Kwong, and P. A. Loach, *J. Heterocycl. Chem.*, **13**, 717 (1976); J. L. Y. Kong and P. A. Loach, *J. Heterocycl. Chem.*, **17**, 737 (1980); R. G. Little, J. A. Anton, and P. A. Loach, *J. Heterocycl. Chem.*, **12**, 343 (1975).

13) J. R. Lindsey-Smith and P. R. Sleath, *J. Chem. Soc., Perkin Trans. 2*, **1982**, 1009; A. W. van der Made, E. J. H. Hoppenbrouwer, R. J. M. Nolte, and W. Drenth, *Recl. Trav. Chim. Pays-Bas*, **107**, 15 (1988).

14) J. A. Runquist and P. A. Loach, *Biochem. Biophys. Acta*, **637**, 231 (1981).

15) F. Ojima, N. Kobayashi, and T. Osa, *Bull. Chem. Soc. Jpn.*, **63**, 1374 (1990); H. Fujii, *J. Am. Chem. Soc.*, **115**, 4641 (1993).

16) M. Nango, K. Iida, K. Yamashita, K. Tsuda, Y. Ohtsuka, and M. Nakata, "The 3rd SPSJ International Polymer Conference," Nagoya, Japan, November 1990, Abstr. No. 28D13.

17) M. Nango, H. Kryu, and P. A. Loach, *J. Chem. Soc., Chem. Commun.*, **1988**, 697.

18) H. Tamiaki, K. Nomura, and K. Maruyama, *Bull. Chem. Soc. Jpn.*, **67**, 1863 (1994).

19) K. Iida, M. Nango, M. Yamaguchi, H. Kasagi, K. Yamashita, K. Tsuda, A. Mizusawa, T. Miyake, A. Masuda, and J. Yoshinaga, submitted.